International Forum on Aeroelasticity and Structural Dynamics
IFASD 2022
13-17 June 2022, Madrid, Spain

TOW-STEERED AEROELASTIC TAILORING FOR IMPROVED HORIZONTAL STABILISER PERFORMANCE

Ronald C. M. Cheung[1], Djamel Rezgui[1], Jonathan E. Cooper[1], Richard B. Green[2] and Raul C. Llamas-Sandin[3]

[1] University of Bristol
Department of Aerospace Engineering,
Queens Building, University Walk, Bristol BS8 1TR, UK
r.c.m.cheung@bristol.ac.uk

[2] University of Glasgow
Aerospace Sciences Division, School of Engineering
James Watt Building South, Glasgow G12 8QQ, UK
richard.green@glasgow.ac.uk

[3] AIRBUS OSL
Av. John Lennon s/n, 28096 Getafe, Spain.
raul.c.llamas@airbus.com

Keywords: Aeroelastic tailoring, tow-steered composites, horizontal stabiliser.

Abstract: Aeroelastic tailoring based on tow-steered composites is applied to the structural design of a horizontal stabiliser. The lift-curve slope of the stabiliser is viewed as the primary performance measure in this work and the aim of the aeroelastic tailoring process is to increase it, with consideration to the stabiliser in a forward, zero or backward-swept configuration. The tow-steered design is compared to a structurally stiff baseline as well as an aeroelastically tailored unidirectional design. It is shown that the use of tow-steered composites can improve the lift-curve slope in all sweep configurations, as well as resulting in designs that can distribute stresses more evenly under load. Furthermore, the tow-steered design enables an additional gain of 3.8% in lift-curve slope beyond the optimal unidirectional ply design.

1 INTRODUCTION

In a conventional aircraft, the lift-curve slope of the horizontal stabiliser is a key attribute to the overall stability of the aircraft [1]. A higher lift-curve slope allows the horizontal stabiliser to reduce in size and still achieving the required performance, leading to lower drag and overall aircraft weight. For a conventional backward-swept horizontal stabiliser, a reduction in lift-curve slope occurs due to bend-twist coupling under aerodynamic load. The current research aims to address this shortcoming through aeroelastic tailoring, to favourably alter the aeroelastic behaviour of the horizontal stabiliser and achieve an improved flexible lift-curve slope.

Aeroelastic tailoring using conventional unidirectional plies has been demonstrated in past studies to enable improved performance for wings, ranging from increased flutter and divergence speed [2, 3] to reduced gust and manoeuvre loads [4]. Aeroelastic tailoring can achieve these enhancements through exploiting the anisotropic property of individual unidirectional ply and optimises the layup for the desired directional stiffness. With the advent of tow-steered composites [5], in which the fibres within the composite may be laid following curve lines instead of the conventional straight and parallel, the range of feasible fibre arrangements is widened for achieving the optimal directional stiffness.

The work described in this paper focuses on assessing the potential performance gain using tow-steered composites for aeroelastic tailoring when applied to a horizontal stabiliser. This work has been conceived to complement ongoing wind tunnel testing in demonstrating aeroelastic tailoring for enhancing horizontal stabilisers [6], as per the CleanSky2 project TailSurf. Therefore, the current work references the optimised unidirectional design used for the wind tunnel model construction and assesses any potential improvements by utilising tow-steered composites, while keeping the same primary design objective in maximising the lift-curve slope of the horizontal stabiliser and design constraints. This work also investigates the effectiveness of aeroelastic tailoring in the presence of planform sweep, as it follows the wind tunnel studies as shown in Figure 1.

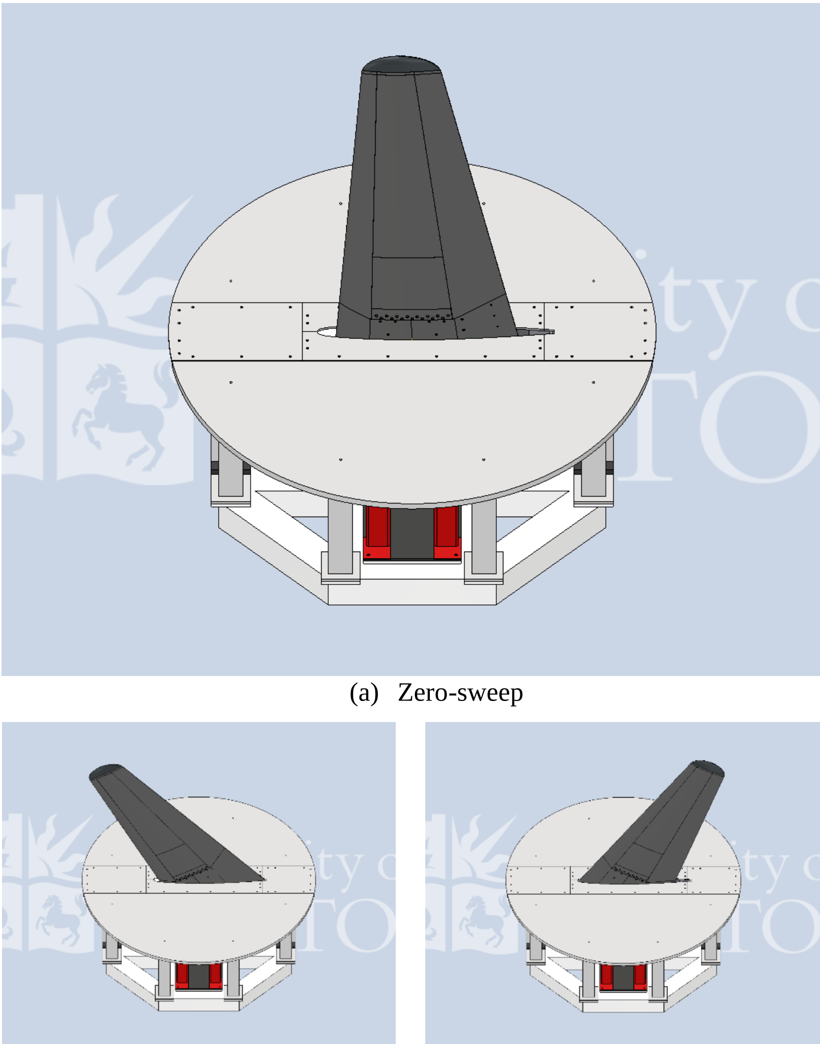

(a) Zero-sweep

(b) 30-deg forward-swept

(c) 30-deg backward-swept

Figure 1: Wind tunnel test configurations.

2 AEROELASTIC TAILORING

The horizontal stabiliser wind tunnel model [6] that this work is based upon has a span of 1.60m with a mean aerodynamic chord of 0.55m and a taper ratio of 0.405. This wind tunnel model is sized such that it can be effectively tested up to a Reynolds number of 1.94×10^6, or a wind tunnel velocity of 50m/s, in all sweep configurations. Figure 2 shows the NASTRAN finite element model (FEM) of this wind tunnel model, which is used as the platform for aeroelastic predictions in this work. The FEM consists of a structural representation of the wing box and an aerodynamic mesh for the Doublet Lattice Method (DLM) [7] for aeroelastic computations. The FEM is available in two versions, an un-optimised baseline and an aeroelastically tailored design, both using unidirectional plies in its wing box construction. Therefore, potential performance gained through using tow-steered composites may be established by comparing the predictions against these two models. The comparison against the already optimised unidirectional composite design is crucial in determining the potentials of tow-steering composites over the conventional approach.

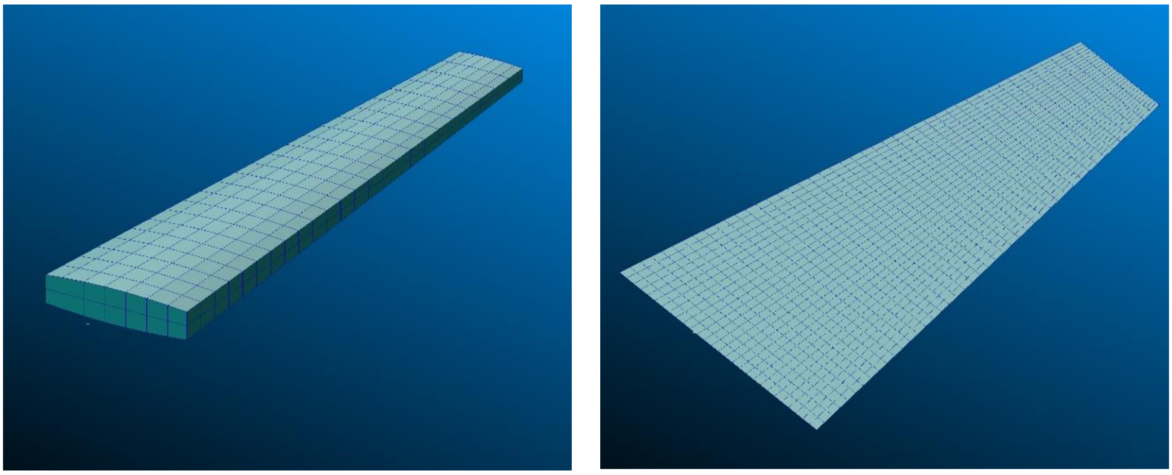

(a) Wing box (b) DLM aerodynamic mesh

Figure 2: NASTRAN FEM of the horizontal stabiliser.

The physical wing box is constructed using carbon fibre wrapped over a foam core, and thus the finite element model represents this arrangement using a combination of shell elements for the composite layup and hexahedral elements for the foam core. The aeroelastic tailoring process then uses the built-in optimisation routine SOL200 in NASTRAN to determine the optimal design of the composite layup in these shell elements.

The physical properties of the materials used for the wing box are provided in Table 1, which are reflected in the material definitions of the FEM. From the table, the spar ply refers to the material used for the upstream and downstream face of the constructed wing box.

Table 1: Composite material properties.

Part	Material	Ply thickness (cured), mm	Density, kg/m^3	Elastic modulus, GPa	In-plane shear modulus, GPa
Foam core	UNE EN 13164	-	39	0.013	0.0045
Skin ply (Warp direction)	AIMS 05-04-100	0.262	1600	130.0	4.0
Skin ply (Weft direction)	AIMS 05-04-100	0.262	1600	9.5	4.0
Spar ply (Fibre direction)	Hexforce G0904 D 1070	0.200	1530	65.0	4.0

In order to represent the tow-steered composites effectively, the ply orientation in each shell element is described using a shape function. The shape function is chosen such that sufficient continuity is maintained across each shell element boundary. This approach is necessary as the tow-steered fibres are continuous and physically limited by a minimum curvature. In this study, the shape function is an nth-order polynomial based on the spanwise position, y, of each shell element.

$$\theta = \sum_{i=0}^{n} a_i y^i \quad (1)$$

The optimiser is tasked to determine the coefficients, a, to this polynomial, such that the objective function returns the highest value, as it corresponds to the design that gives the steepest lift-curve slope. Using this formulation, a unidirectional ply can also be represented by reducing this shape function down to 0th-order.

A unidirectional design was obtained from a previous part of this work [6], in which optimisation took place to determine the coverage of the inner skin ply. As shown in Table 2, the inner ply only covers the first 20.8% of the span of the wing box from the root. This configuration was necessary to allow the wing box to deform sufficiently in wind tunnel test condition. Since the motivation for this tow-steering optimisation is to demonstrate further gains in performance, the optimisations detailed in this paper are thus only applied to the outer ply, while the inner ply coverage and orientation remaining the same. The fibre orientation used in this work is an angular measurement from the mid-chord line and anticlockwise positive when observed from outside the wing box.

Table 2: Comparison of wing box construction.

Wing box design	Upper skin inner ply span, %	Upper skin inner ply θ, deg	Upper skin outer ply θ, deg	Lower skin inner ply span, %	Lower skin inner ply θ, deg	Lower skin outer ply θ, deg
Baseline	100.0	0.0	0.0	100.0	0.0	0.0
Unidirectional	20.8	-19.6	Constant	20.8	19.6	Constant
Tow-steered	20.8	-19.6	5th-order polynomial	20.8	19.6	5th-order polynomial

3 RESULTS

The aeroelastic tailoring process optimises the tow-steering angle for the outer skin ply of the composites in the pressure and suction side of the wing box. This approach is similar to the process that had taken place to produce the optimised unidirectional composite design, making the tow-steered composite design directly comparable. Therefore, the material definitions, stress limits and design constraints are also kept the same. The tow-steer angle shape function is chosen to be 5th order, whilst the ply thickness is kept constant.

Table 3: Material stress limits.

Part	Material	Tensile limit, MPa	Compressive limit, MPa	In-plane limit, MPa
Foam core	UNE EN 13164	0.5	0.3	0.2
Skin ply (Warp direction)	AIMS 05-04-100	1160.0	308.0	80.0
Skin ply (Weft direction)	AIMS 05-04-100	32.0	70.0	80.0
Spar ply (Fibre direction)	Hexforce G0904 D 1070	700.0	670.0	80.0

As the follow-on work from previous research, the horizontal stabiliser is considered in three sweep configurations for investigating the effectiveness of combining the aeroelastic from planform change with aeroelastic tailoring. These configurations are 30-deg forward, zero and 30-deg backward-swept. An optimisation is run separately in each sweep configuration, with the optimiser set to maximise lift at 10-deg angle of attack and wind tunnel velocity of 50 m/s, while respecting a structural safety factor of 2.0 based on the material stress limits listed in Table 3. With additional constraint is applied to ensure the lift-curve is symmetric about zero angle of attack, maximising lift in this manner fulfils the underlying objective of maximising the lift-curve slope.

The unidirectional design in the 30-deg forward-swept configuration is the exact design used in the constructed wind tunnel model, which had already undergone the aeroelastic tailoring process. For the zero and 30-deg backward-swept configurations, a new optimised solution is sought individually for a direct comparison against the tow-steered design of the corresponding configurations.

3.1 Static aeroelastic performance

Static aeroelastic predictions are obtained using SOL144 in NASTRAN at the same flight condition of 50m/s and 10-deg angle of attack as the aeroelastic tailoring design condition. The lift-curve is assumed linear and the corresponding lift-curve slope values are listed in Table 4.

Table 4: Comparison of static aeroelastic results.

	Lift-curve slope, rad^{-1}		
Wing box design	30-deg forward-swept	Zero-Sweep	30-deg backward-swept
Baseline	3.763	4.577	3.821
Unidirectional	4.472 (+18.8%)	5.029 (+9.9%)	4.068 (+6.5%)
Tow-steered	4.530 (+20.4%)	5.203 (+13.7%)	4.077 (+6.7%)

From Table 4, the static aeroelastic prediction using tow-steered composites is shown to produce up to 20.3% increase in lift-curve slope when compared with the baseline, which means the size of the horizontal stabiliser could potentially reduce without affecting aircraft performance. It is important to note that the tow-steered designs are better performing than the unidirectional designs, with up to an additional 3.8% improvement. It should be noted that the zero-sweep lift-curve slope is generally higher than the other sweep configurations because the effective aspect ratio is the highest in this configuration.

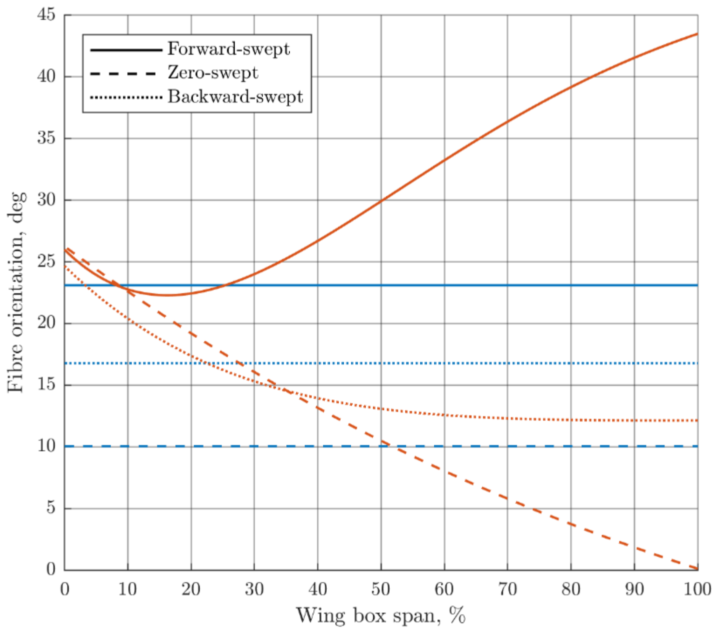

Figure 3: Optimal solutions of the lower skin ply (unidirectional design in blue, tow-steered design in red).

From the optimal solutions shown in Figure 3, the fibres are generally orientated further towards the backward wing-sweep direction. Orienting fibres in this direction encourages a nose-up twist of the wing box under lifting loads, which in turn increases the lift generated by the stabiliser. This aeroelastic effect can be seen in Figure 4, where both the tow-steered and unidirectional composite designs have significant increase in nose-up spanwise twist distribution when compared to the baseline.

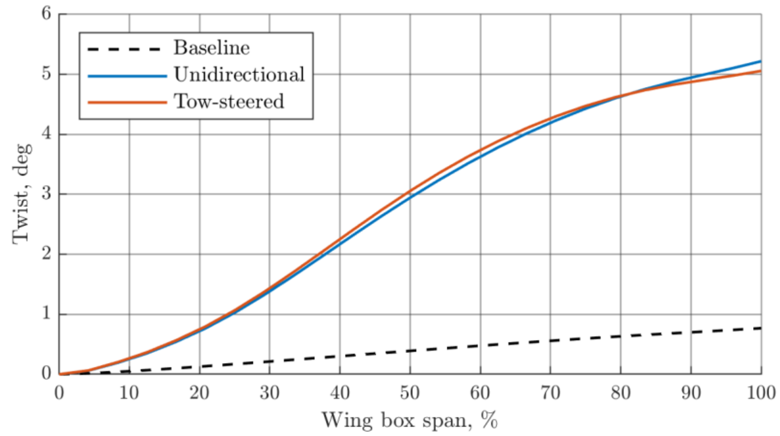

(a) 30-deg forward-swept

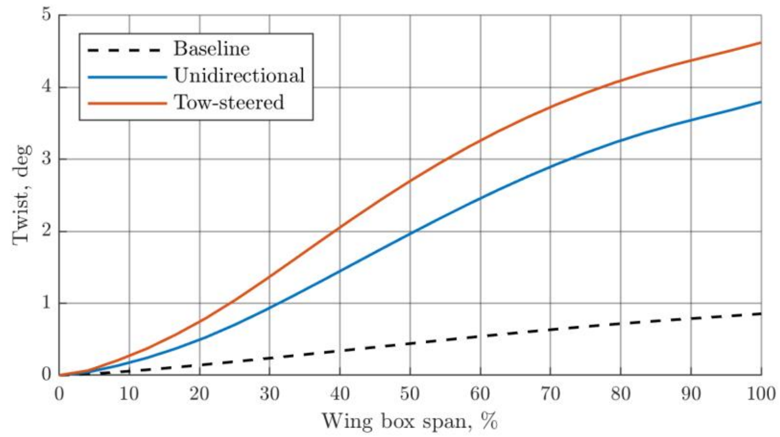

(b) Zero-sweep

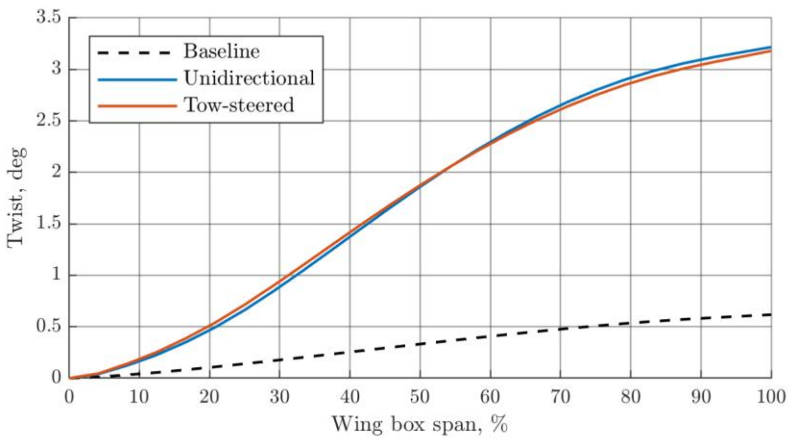

(c) 30-deg backward-swept

Figure 4: Wing box twist with respect to mid-chord line at 50m/s with 10-deg angle of attack.

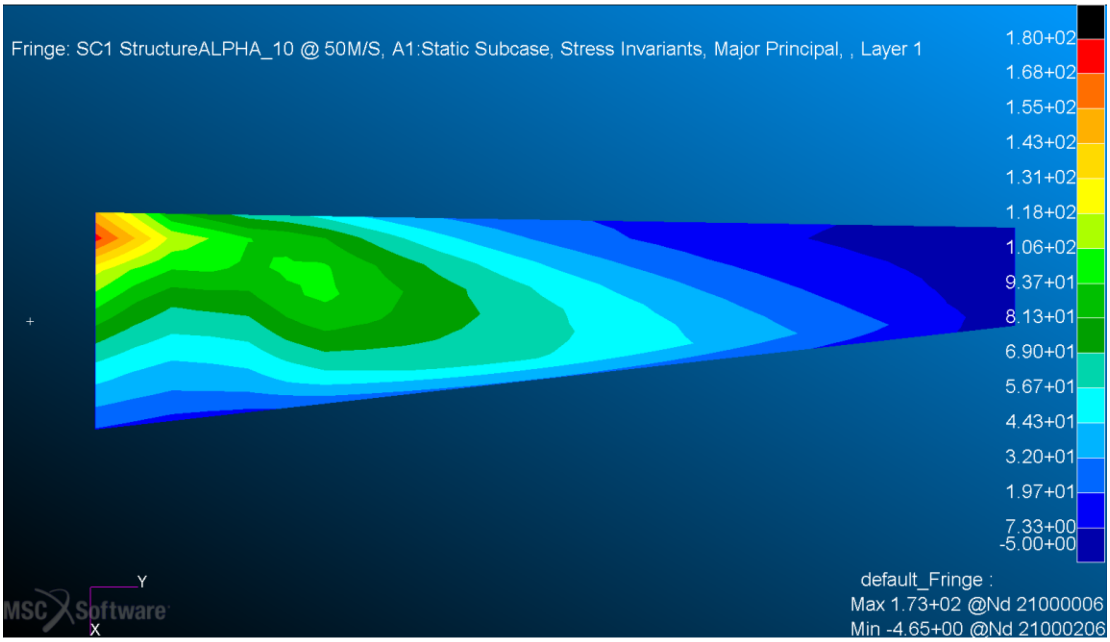

(a) Unidirectional design

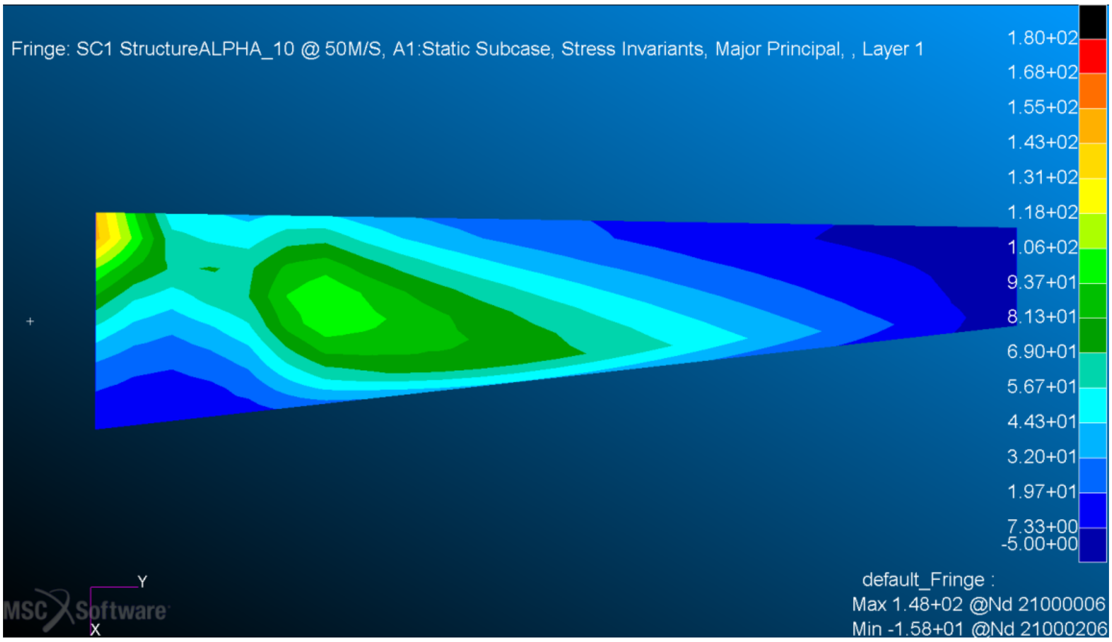

(b) Tow-steered design

Figure 5: Major principal stress distribution in the outer skin ply in the zero-sweep configuration (50m/s with 10-deg angle of attack).

For the forward and backward-swept cases, as shown in Figure 4(a) and (c) respectively, the difference in the spanwise fibre orientations manifests into higher mid-span twist in the tow-steered design. Despite lower twist at the wingtip, the result is a net gain in lift due to the tapered planform. In the zero-sweep configuration as shown in Figure 4(b), the tow-steered design can generate higher twist along the span, and therefore a higher overall lift. Figure 5(a) shows that the stress concentration near the junction between the wing root and front spar is the limiting constraint for the unidirectional design in this sweep configuration. For the tow-steered design, as illustrated in Figure 5(b), the additional degrees of freedom in varying the fibre orientation allows the stress concentration to be lowered, as well as distributing more loading to the mid-span area to achieve a higher overall lift. This observation is also evident in Figure 6, which shows the tow-steered design exploits the allowable strain more effectively in the mid-span region.

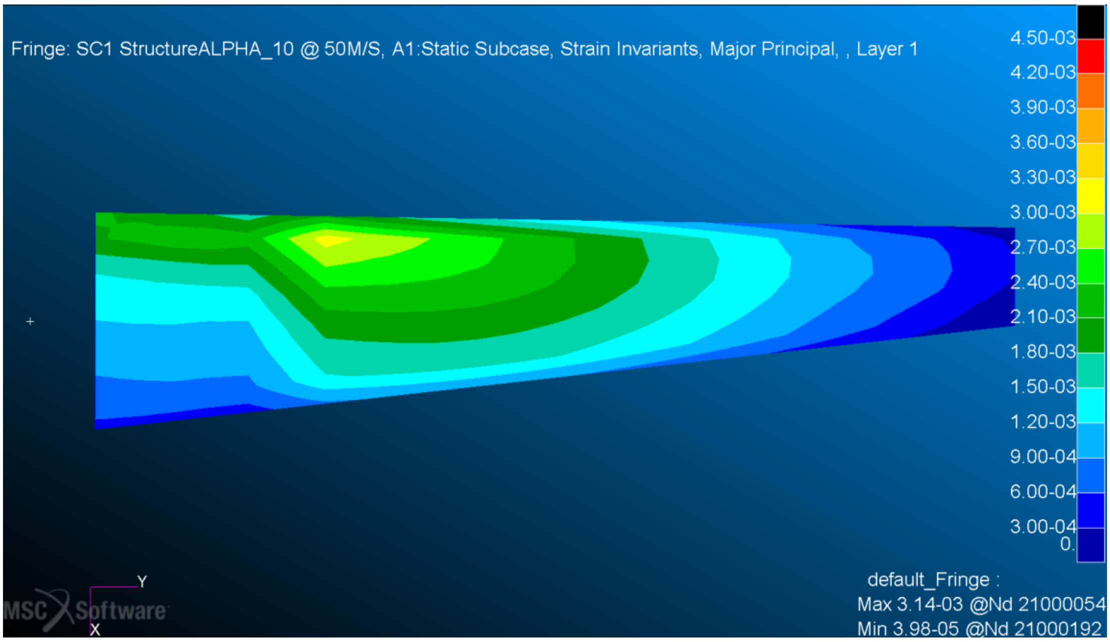

(a) Unidirectional design

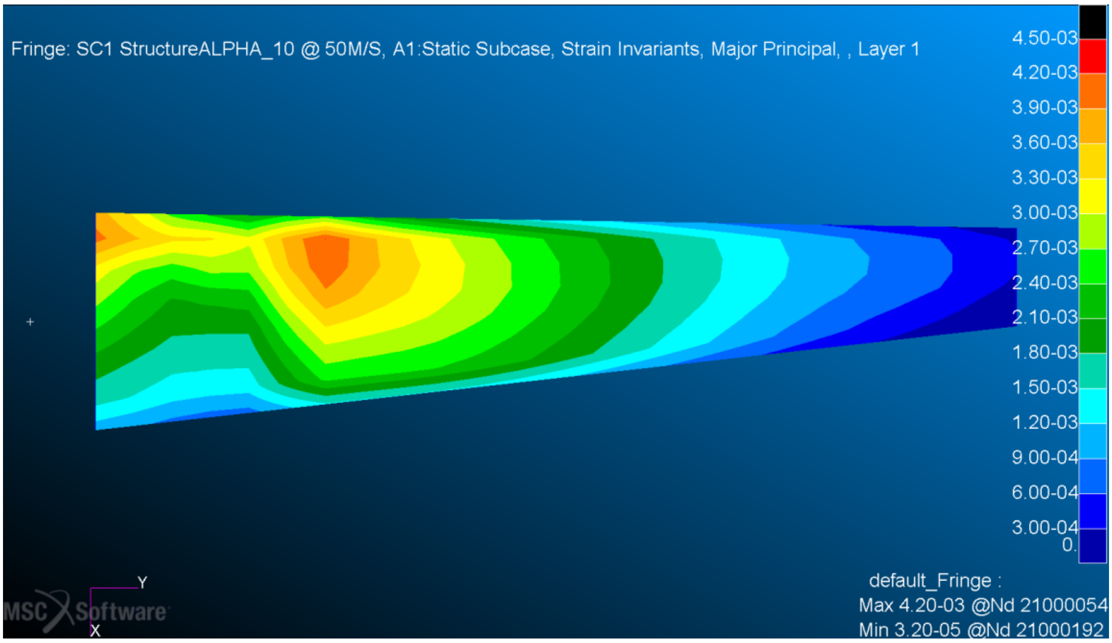

(b) Tow-steered design

Figure 6: Major principal strain distribution in the outer skin ply in the zero-sweep configuration (50m/s with 10-deg angle of attack).

3.2 Flutter analysis

Dynamic behaviour of each design is analysed using SOL145 in NASTRAN through the PK method. Structural damping parameter in these computations is set to 1%, making them more conservative when compared to the typical value of 2% used in structural dynamics. Frequency and damping trends from these computations are shown in Figure 7 to Figure 9 for each design and sweep configuration. In these figures, aeroelastic instabilities are identified when the damping ratio margin first becomes positive. The zero-velocity modeshape of these unstable modes are shown in Figure 10 to Figure 12, along with the instability speed margins summarised in Table 5.

Table 5: Comparison of instability speed margins.

	Instability speed margin (based on design velocity of 50m/s)		
Wing box design	30-deg Forward-swept	Zero-Sweep	30-deg Backward-swept
Baseline	77.8% (Divergence)	78.9% (Divergence)	81.2% (Flutter)
Unidirectional	46.5% (Divergence)	58.4% (Divergence)	70.5% (Divergence)
Tow-steered	44.7% (Divergence)	54.3% (Divergence)	69.9% (Divergence)

From Table 5, except for the baseline design in the backward-swept configuration, flutter is a non-issue as divergence is predicted to occur at a lower speed. A general trend observed in these divergence speeds is a reduction towards a forward-swept configuration, which agrees well with the classical explanation of bend-twist coupling in flexible forward-swept wings. As seen in Figure 4, the optimised designs exploit this aeroelastic effect further to increase lift with a higher spanwise nose-up twist distribution. Therefore, it is within expectation that lower divergence speed margins are reported in Table 5. In addition, the bend-twist dominate instability modeshapes shown in Figure 10 to Figure 12 reinforce this explanation further. For the backward-swept configuration, it is important to note that the divergence speed now dips below the flutter speed and becomes the critical instability.

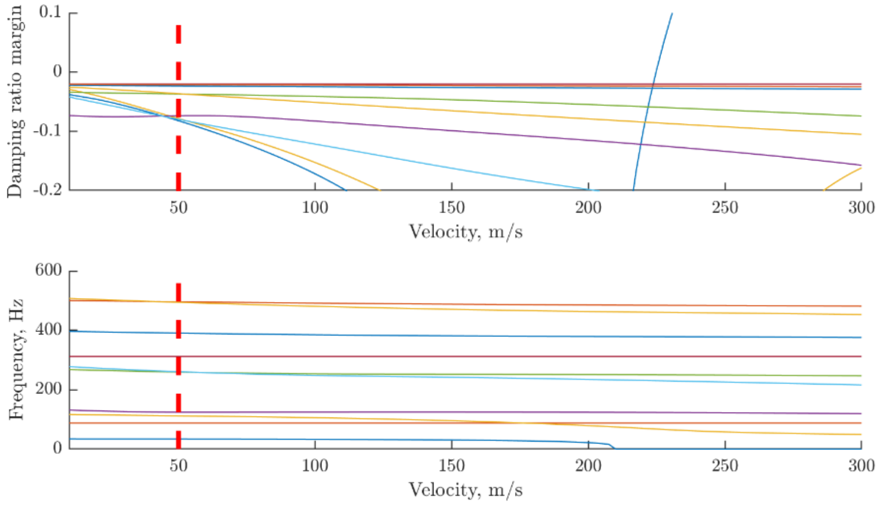

(a) Baseline

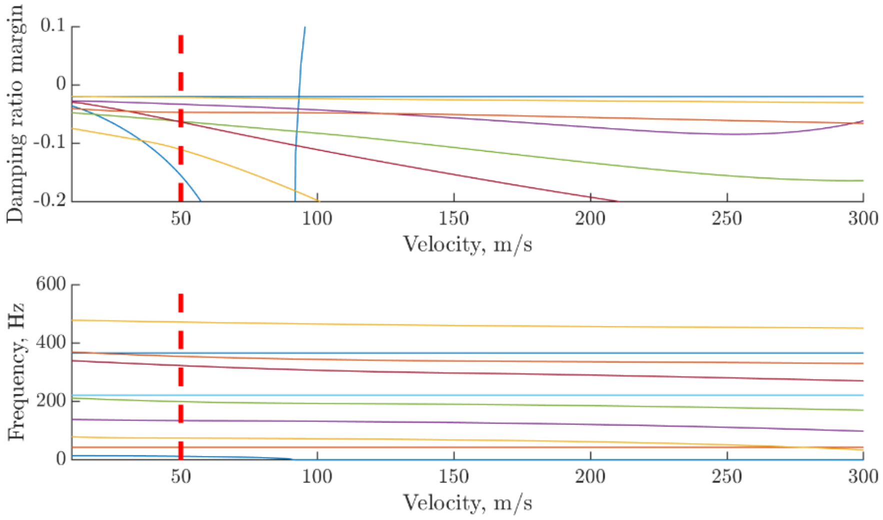

(b) Unidirectional design

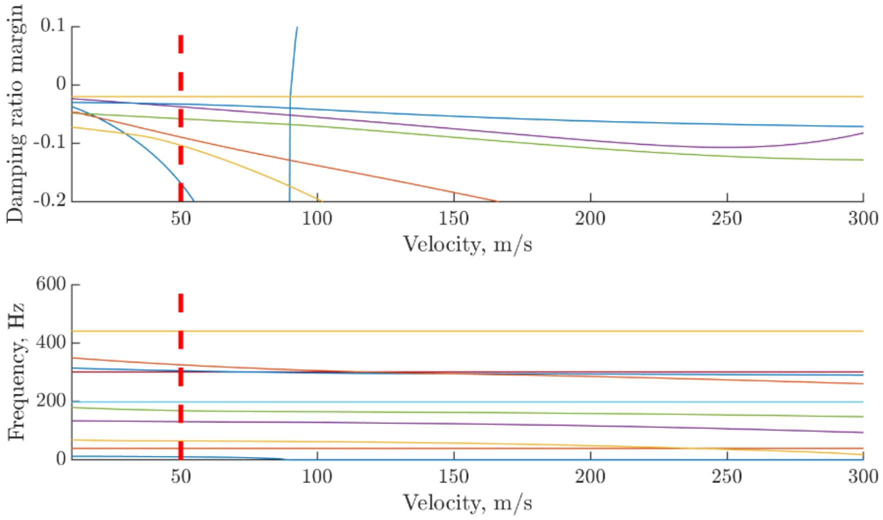

(c) Tow-steered design

Figure 7: Flutter analysis results – 30-deg forward-swept (design velocity shown as red broken line).

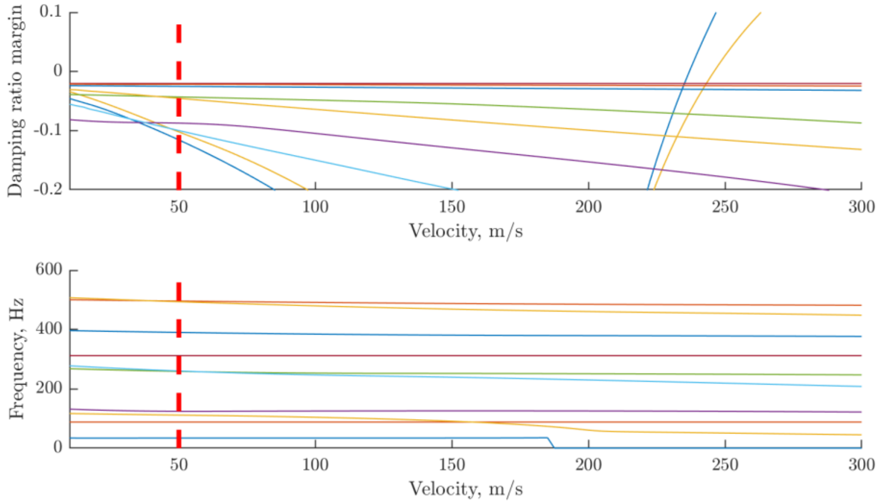

(a) Baseline

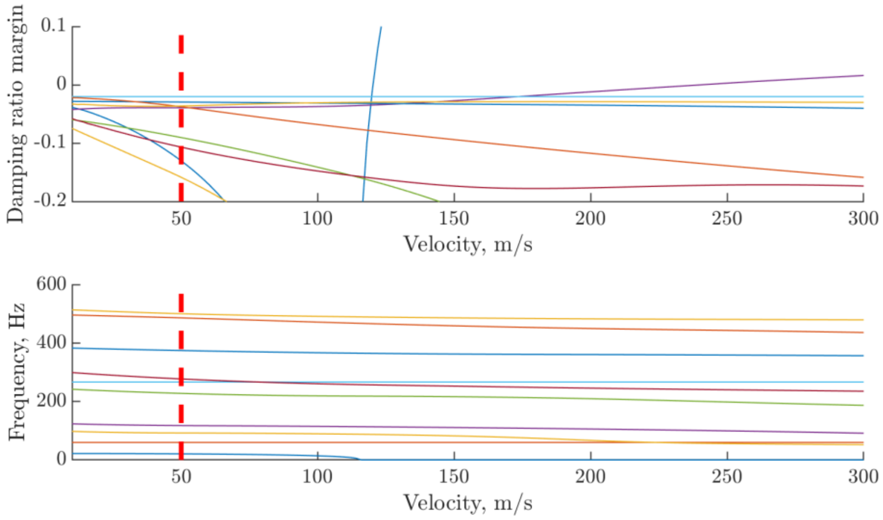

(b) Unidirectional design

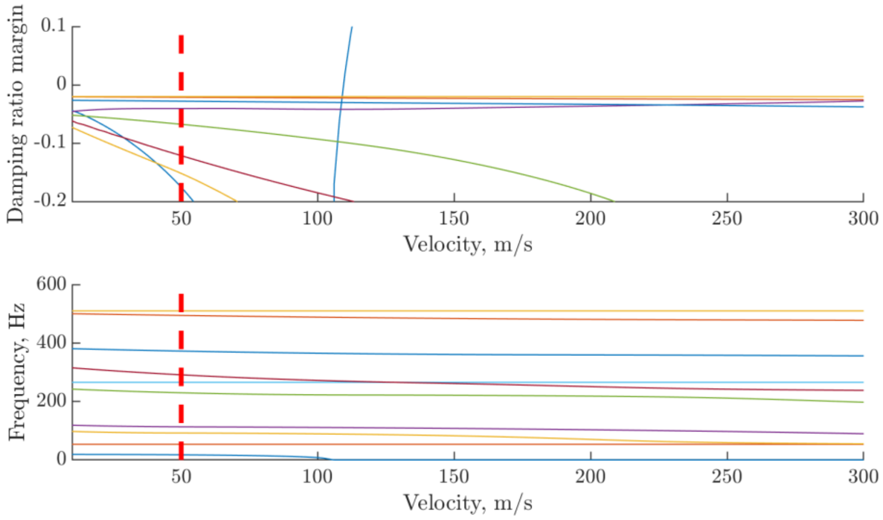

(c) Tow-steered design

Figure 8: Flutter analysis results – zero-sweep (design velocity shown as red broken line).

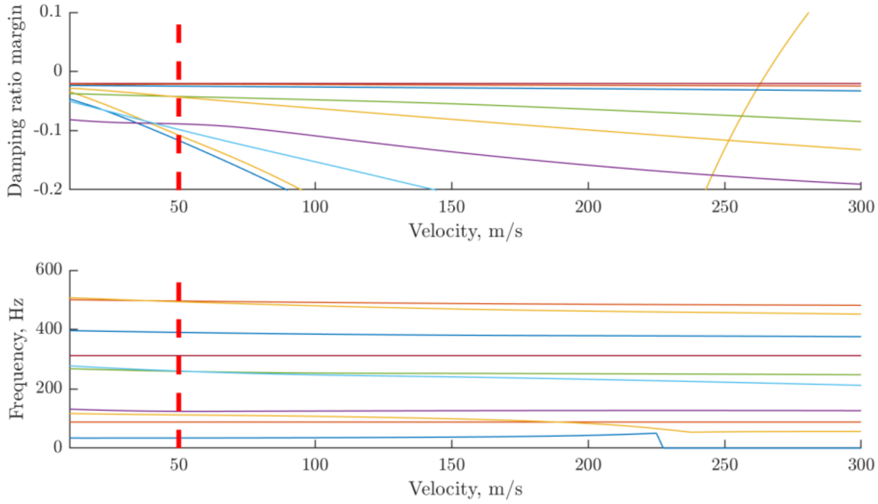

(a) Baseline

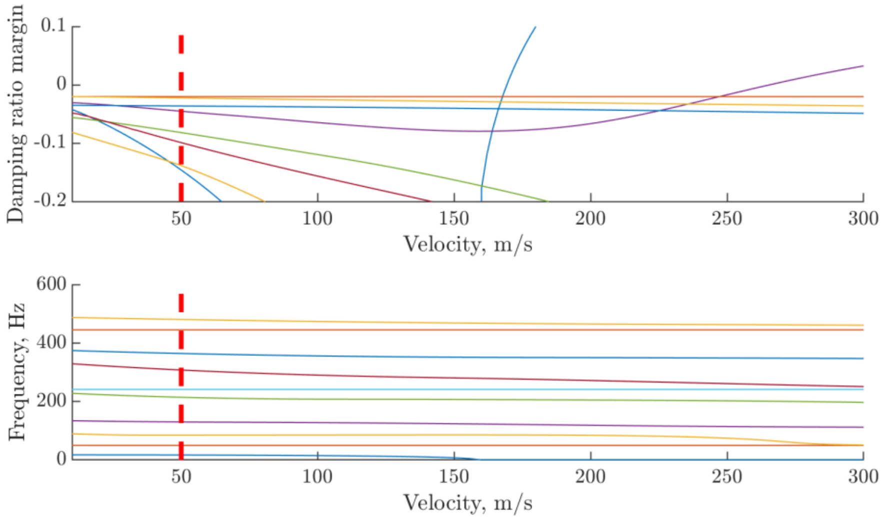

(b) Unidirectional design

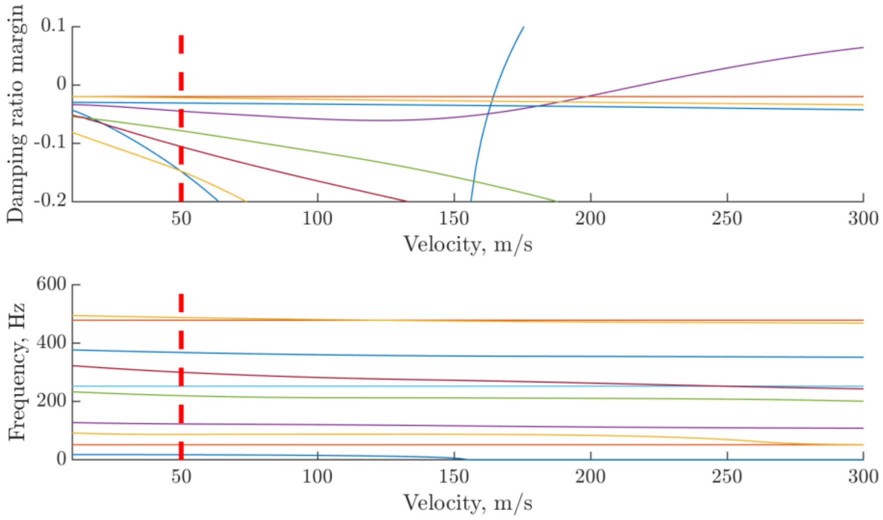

(c) Tow-steered design

Figure 9: Flutter analysis results – 30-deg backward-swept (design velocity shown as red broken line).

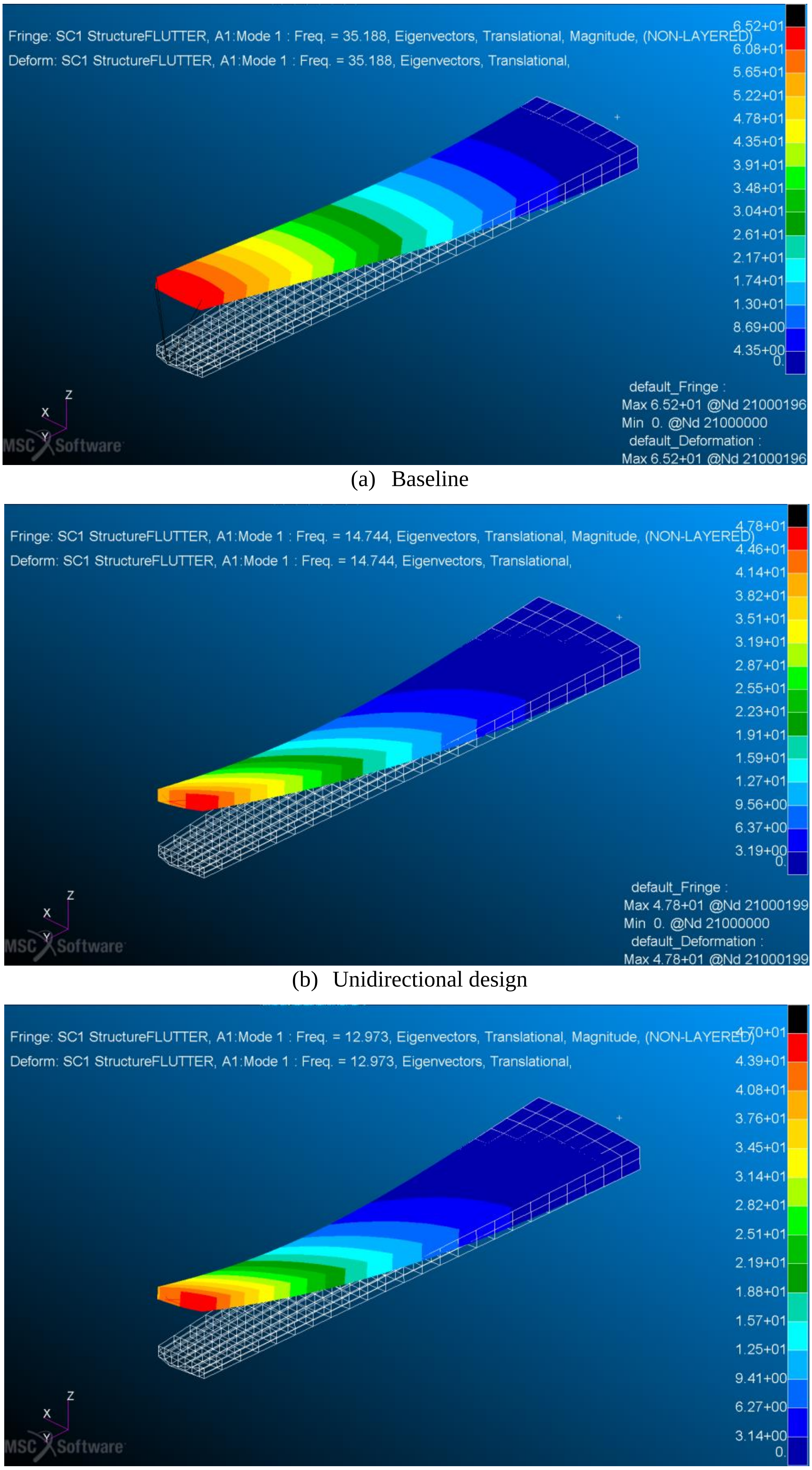

(a) Baseline

(b) Unidirectional design

(c) Tow-steered design

Figure 10: Modeshape of the unstable mode for the 30-deg forward-swept configuration.

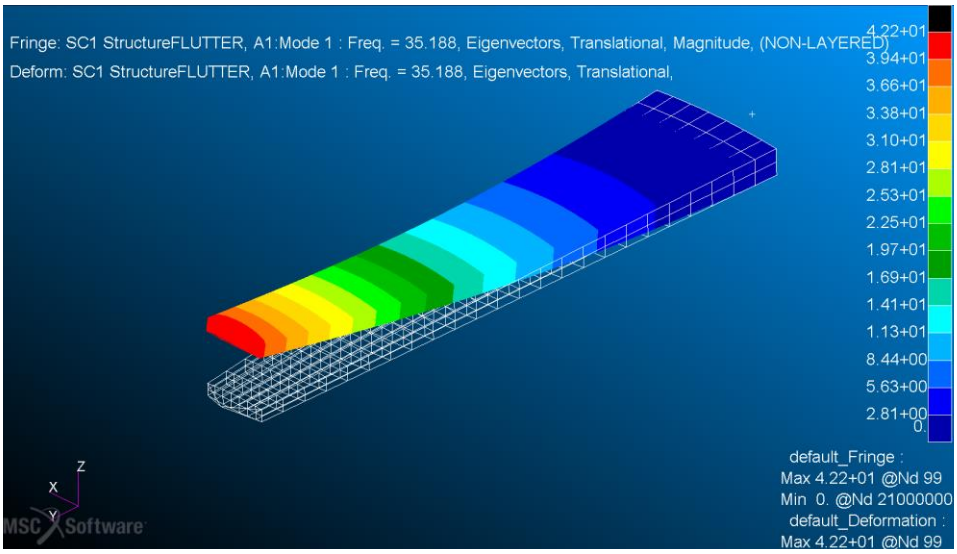

(a) Baseline

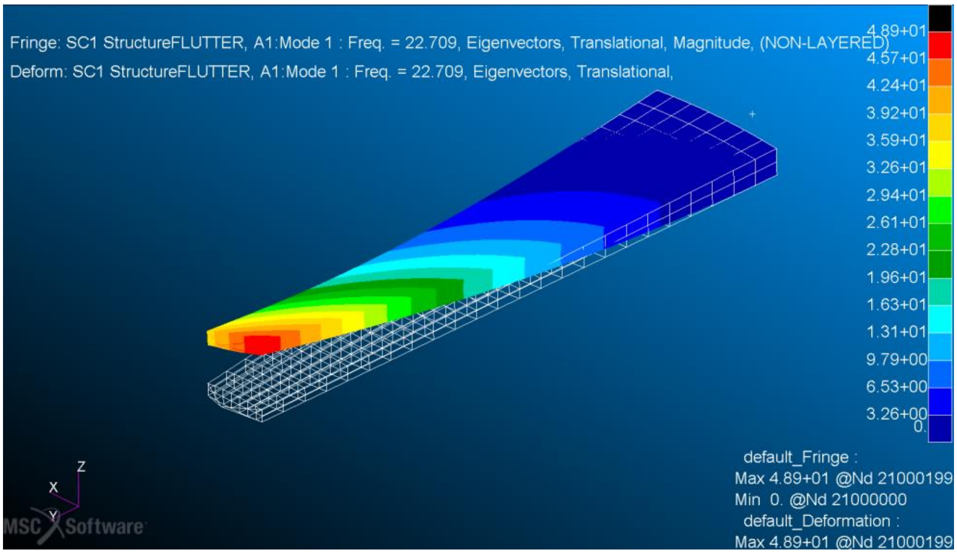

(b) Unidirectional design

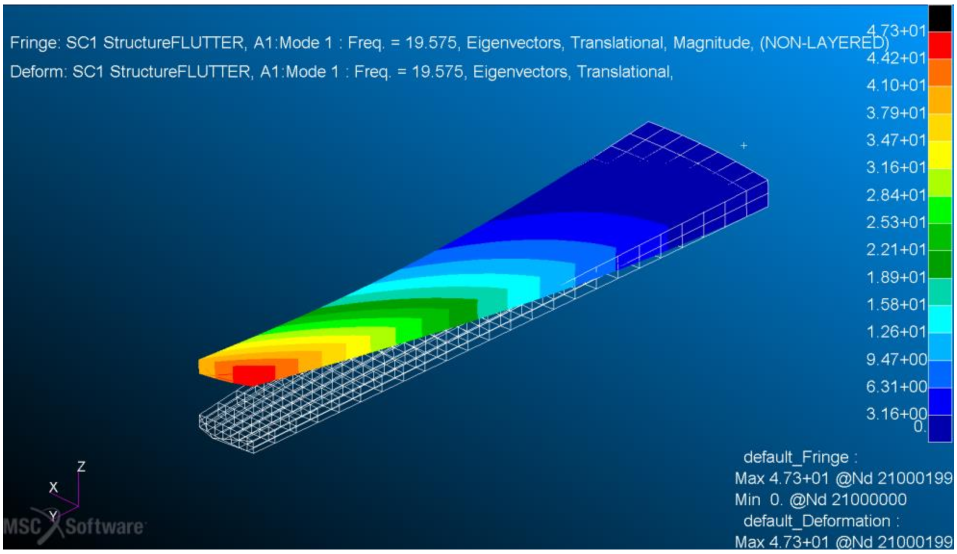

(c) Tow-steered design

Figure 11: Modeshape of the unstable mode for the zero-sweep configuration.

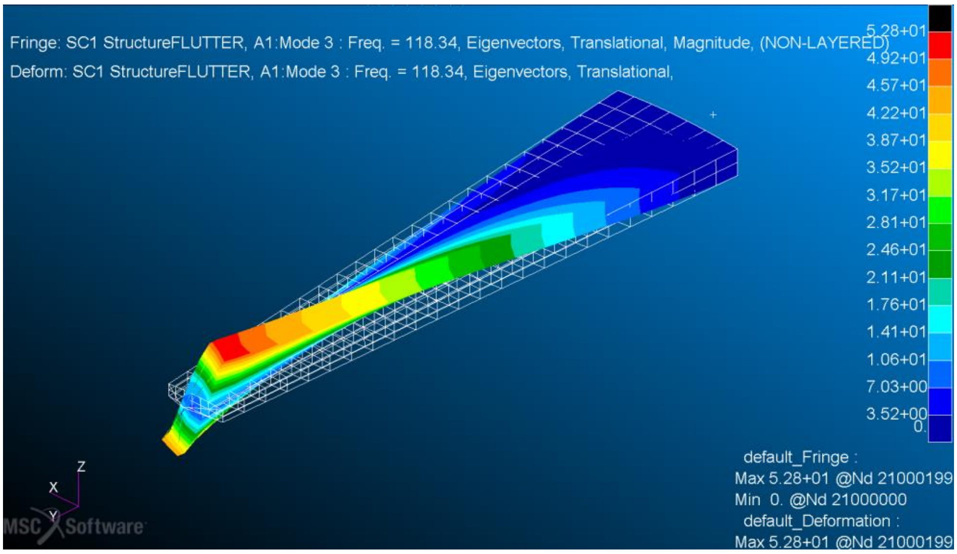

(a) Baseline

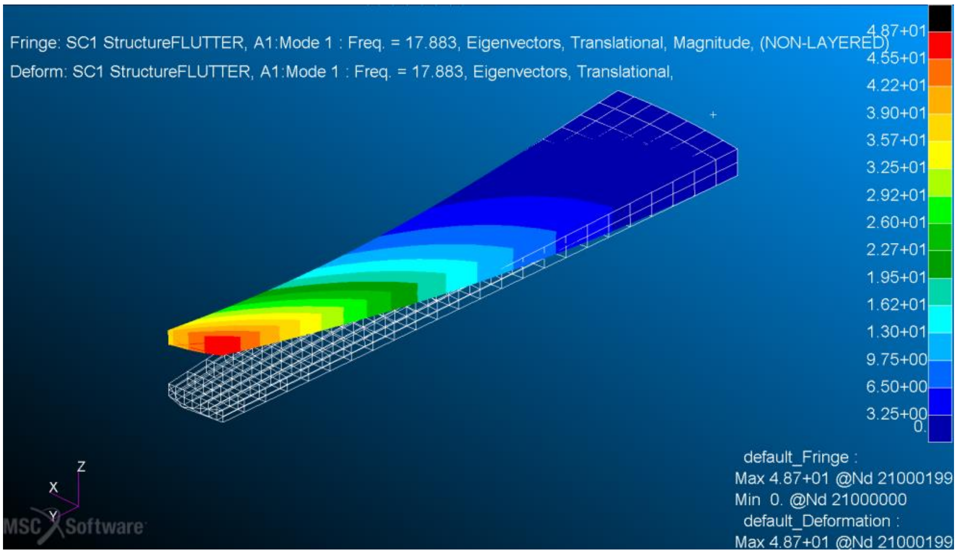

(b) Unidirectional design

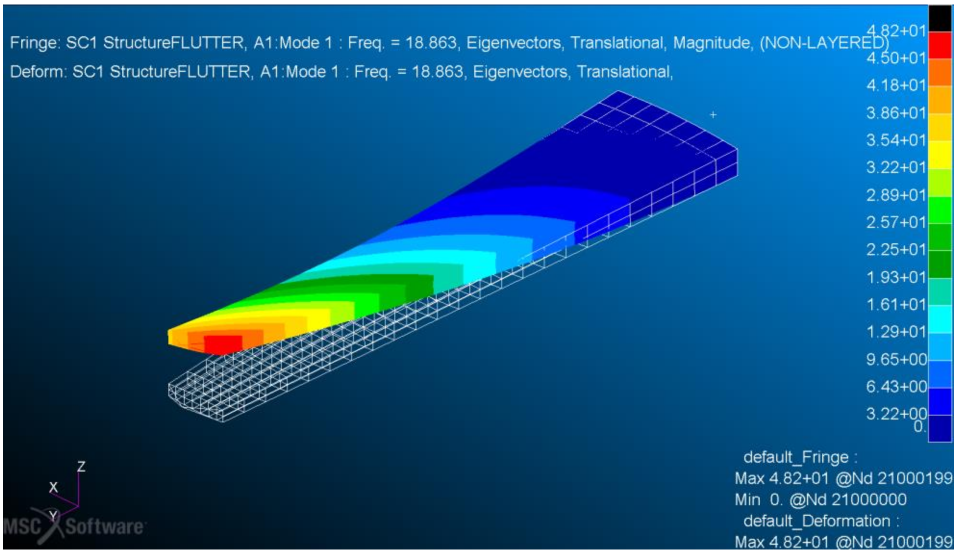

(c) Tow-steered design

Figure 12: Modeshape of the unstable mode for the 30-deg backward-swept configuration.

4 CONCLUSIONS

Aeroelastic tailoring has been applied to optimise the composite construction of a horizontal stabiliser model to be tested in a wind tunnel. The design objective is to increase the lift-curve slope of the stabiliser when in a forward, zero or backward-swept configuration. Designs utilising conventional unidirectional and tow-steered composites are considered in this study and implemented as finite element models in NASTRAN for aeroelastic optimisation. Static and dynamic aeroelastic analyses are also conducted using these finite element models to establish the performance difference between these designs, as well as against a structurally stiff baseline. The conventional unidirectional composite layup is shown to be effective for all three sweep configurations, with up to 18.8% improvement from the baseline design. However, it is demonstrated that tow-steered composites can allow for more even distribution of stresses under load, which enables an additional gain of 3.8% beyond the optimal unidirectional ply solution. The lift benefit observed is found to be associated with the increased spanwise twist of the stabilisers. Although all configurations are stable within the design velocity envelope, the stability margins are reduced for the aeroelastically tailored designs. Divergence is also found to be more critical than flutter for the backward-swept configuration when compared to the baseline design.

5 ACKNOWLEDGEMENTS

This research is conducted as part of the project titled: Rear End Aerodynamic and Aeroelastic Studies (Grant Agreement No: 864290). The partners in this project are Airbus, University of Nottingham, University of Bristol and University of Glasgow.

6 REFERENCES

[1] Roskam, J. *Airplane Design (Part III:Layout Design of Cockpit, Fuselage, Wing and Empennage: Cutaways and Inboard Profile)*, DAR Corporation, Kansas, USA, 2002.

[2] Stodieck, O., Cooper, J. E., Weaver, P. M., and Kealy, P. "Improved aeroelastic tailoring using tow-steered composites," *Composite Structures* Vol. 106, 2013, pp. 703-715.doi: https://doi.org/10.1016/j.compstruct.2013.07.023

[3] Weisshaar, T. A. "Aeroelastic Tailoring of Forward Swept Composite Wings," *Journal of Aircraft* Vol. 18, No. 8, 1981, pp. 669-676.doi: 10.2514/3.57542

[4] Kim, T.-U., and Hwang, I. H. "Optimal design of composite wing subjected to gust loads," *Computers & Structures* Vol. 83, No. 19, 2005, pp. 1546-1554.doi: https://doi.org/10.1016/j.compstruc.2005.02.002

[5] Kim, B. C., Potter, K., and Weaver, P. M. "Continuous tow shearing for manufacturing variable angle tow composites," *Composites Part A: Applied Science and Manufacturing* Vol. 43, No. 8, 2012, pp. 1347-1356.doi: https://doi.org/10.1016/j.compositesa.2012.02.024

[6] R.C.M. Cheung, D. R., J.E. Cooper, R.B. Green, R.C. Llamas-Sandin. "Improving Horizontal Stabilizer Performance Using Aeroelastic Tailoring," *AIAA Scitech 2022 Forum*, 2022.doi: https://doi.org/10.2514/6.2022-0017

[7] Albano, E., and Rodden, W. P. "A doublet-lattice method for calculating lift distributions on oscillating surfaces in subsonic flows," *AIAA Journal* Vol. 7, No. 2, 1969, pp. 279-285.doi: 10.2514/3.5086

COPYRIGHT STATEMENT